



Racemic *S*-(ethylsulfonyl)-DL-cysteine *N*-Carboxyanhydrides Improve Chain Lengths and Monomer Conversion for β -Sheet-Controlled Ring-Opening Polymerization

Tobias A. Bauer, Christian Muhl, Dieter Schollmeyer, and Matthias Barz*

The secondary structure formation of polypeptides not only governs folding and solution self-assembly but also affects the nucleophilic ring-opening polymerization of α -amino acid-*N*-carboxyanhydrides (NCAs). Whereby helical structures are known to enhance polymerization rates, β -sheet-like assemblies reduce the propagation rate or may even terminate chain growth by precipitation or gelation. To overcome these unfavorable properties, racemic mixtures of NCAs can be applied. In this work, racemic *S*-(ethylsulfonyl)-DL-cysteine NCA is investigated for the synthesis of polypeptides, diblock and triblock copolymer(s). In contrast to the polymerization of stereoregular *S*-(ethylsulfonyl)-L-cysteine NCA, the reaction of *S*-(ethylsulfonyl)-DL-cysteine NCA proceeds with a rate constant of up to $k_p = 1.70 \times 10^{-3} \text{ L mol}^{-1} \text{ s}^{-1}$ and is slightly faster than the enantiopure polymerization. While the polymerization of *S*-(ethylsulfonyl)-L-cysteine NCA suffers from incomplete monomer conversion and degrees of polymerization (DPs) limited to 30–40, racemic mixtures yield polypeptides with DPs of up to 102 with high conversion rates and well-defined dispersities (1.2–1.3). The controlled living nature of the ring-opening polymerization of *S*-(ethylsulfonyl)-DL-cysteine NCA thus enables the synthesis of triblock copolymers by sequential monomer addition. This methodology allows for precise control over DPs of individual blocks and yields uniform triblock copolymers with symmetric molecular weight distributions at a reduced synthetic effort.

derived from specific side or end groups, polypeptides feature the formation of higher ordered secondary structures, which can be mainly divided into either α -helices or β -sheets, with exemptions for proline-type amino acids.^[4] For controlled living NCA polymerization following the normal amine mechanism, secondary structure formation was shown to have a major impact on the polymerization itself, i.e., reaction kinetics and polypeptide solubility as well as polymer analytics.^[1,5–8]

Polymerization of NCAs leading to homopolymers with a high degree of α -helical segments, e.g., *N*- ϵ -(carbobenzoyl)-L-lysine or γ -(benzyl)-L-glutamate (p(L)Glu(OBn)), starts upon initiation and a short induction period with relatively slow polymerization rate, which is displaced by fast and pseudo-first-order kinetics for later stages of the reaction. Early investigations by Lundberg and Doty as well as recent detailed studies by the Cheng group could explain the increased polymerization rate by an occurring transition from a rather β -sheet-like structure to an α -helical growth supporting the addition of NCA monomers

by directed hydrogen bonds and an induced dipole.^[9–11] In this context, for amino acids forming strong β -sheets from homo-oligopeptides, NCA polymerization is slowed down and may even stop during the induction period as a result of precipitation or crystallization.^[12–15] As such, poly(L-alanine) forms α -helical polypeptides at later stages, but strong β -sheets of the L-alanine oligomers, which complicate NCA polymerization leading to broad and bimodal molecular weight distributions.^[16] To mitigate this secondary structure-driven phenomenon, racemic alanine NCA mixtures were employed resulting in the successful synthesis of polyalanine with elevated molecular weights and narrow molecular weight distribution.^[14]

In contrast to per se helix-forming amino acids, branching as well as the presence of a heteroatom (*O/S*) at the β -carbon atom are both known to favor the formation of β -sheets.^[17] NCA polymerizations of isoleucine, valine, threonine, serine, and cysteine, thus, generally suffer from limited access to high molecular weights and narrow dispersities.^[4,5,18] To overcome these limitations, again, racemic NCA mixtures have been employed for valine and isoleucine.^[15,19–21] For polymerization of L-serine, L-threonine, and L-cysteine NCAs, mostly,

T. A. Bauer, Dr. C. Muhl, Dr. D. Schollmeyer, Prof. M. Barz
Johannes Gutenberg University Mainz
Department of Chemistry
Duesbergweg 10-14 55128, Mainz, Germany
E-mail: m.barz@umail.leidenuniv.nl

T. A. Bauer, Prof. M. Barz
Leiden Academic Centre for Drug Research (LACDR)
Leiden University
Einsteinweg 55, Leiden 2333 CC, The Netherlands

The ORCID identification number(s) for the author(s) of this article can be found under <https://doi.org/10.1002/marc.202000470>.

© 2020 The Authors. Published by Wiley-VCH GmbH. This is an open access article under the terms of the Creative Commons Attribution License, which permits use, distribution and reproduction in any medium, provided the original work is properly cited.

The copyright line for this article was changed on 13 October 2020 after original online publication.

DOI: 10.1002/marc.202000470

modifications were introduced to the β -heteroatom either weakening the β -sheet structure or changing the preferred conformation to an α -helix supporting the chain growth.^[20,22–25]

Among the 20 natural amino acids, cysteine takes a unique role due to its ability to stabilize proteins by (bio-) reversible disulfide bonds.^[26,27] To transfer this feature to synthetic polymers for an application as “smart” or stimuli-responsive material, we previously reported on the *S*-alkylsulfonyl protecting group, which allows for nucleophilic amine-initiated polymerization of *S*-(ethylsulfonyl)-*L*-cysteine NCA and consecutive formation of asymmetric disulfide bonds with thiols (soft nucleophiles).^[28,29] Moreover, block copolymers of poly(sarcosine)-*block*-poly(*S*-ethylsulfonyl-*L*-cysteine), so-called polypept(oid)s,^[30,31] could be successfully employed to prepare disulfide crosslinked polymeric micelles and nanohydrogels.^[32] Nevertheless, the polymerization of *S*-(ethylsulfonyl)-*L*-cysteine NCA was shown to be hampered by the formation of antiparallel β -sheets reducing the polymerization rate constants, lowering monomer conversion rates, and limiting accessible molecular weights.^[29]

The aim of this work is now to investigate the nucleophilic ring-opening polymerization of racemic *S*-(ethylsulfonyl)-*D,L*-cysteine NCAs, to analyze the secondary structure of resulting homopolymers and to incorporate these reactive amino acids into triblock copolymers.

To obtain *S*-(ethylsulfonyl)-*D,L*-cysteine NCA (*D,L*-Cys(SO₂Et) NCA), the corresponding amino acid, *S*-(ethylsulfonyl)-*D,L*-cysteine, was synthesized from racemic cysteine hydrochloride by *S*-nitrosation (umpolung reaction) and in situ reaction with sodium ethylsulfinate, similar to previous reports on the *L*-enantiomer compound.^[28,29] The NCA was prepared according to the Fuchs–Farthing method using diphosgene in tetrahydrofuran (THF) (Figure 1a).^[33–35] Melting points of *D,L*-Cys(SO₂Et) NCA (mp = 86–89 °C) were significantly lower, compared to the *L*-enantiomer (mp = 113–115 °C) compound.^[36] From crystallization attempts of the racemic mixture, only crystals of the *D*-enantiomer could be isolated and analyzed by X-ray crystallography (Figures S1–S3, Supporting Information), revealing NCA monomers arranged as an endless chain along the *b*-axis, mediated by N–H...O hydrogen bonds, which

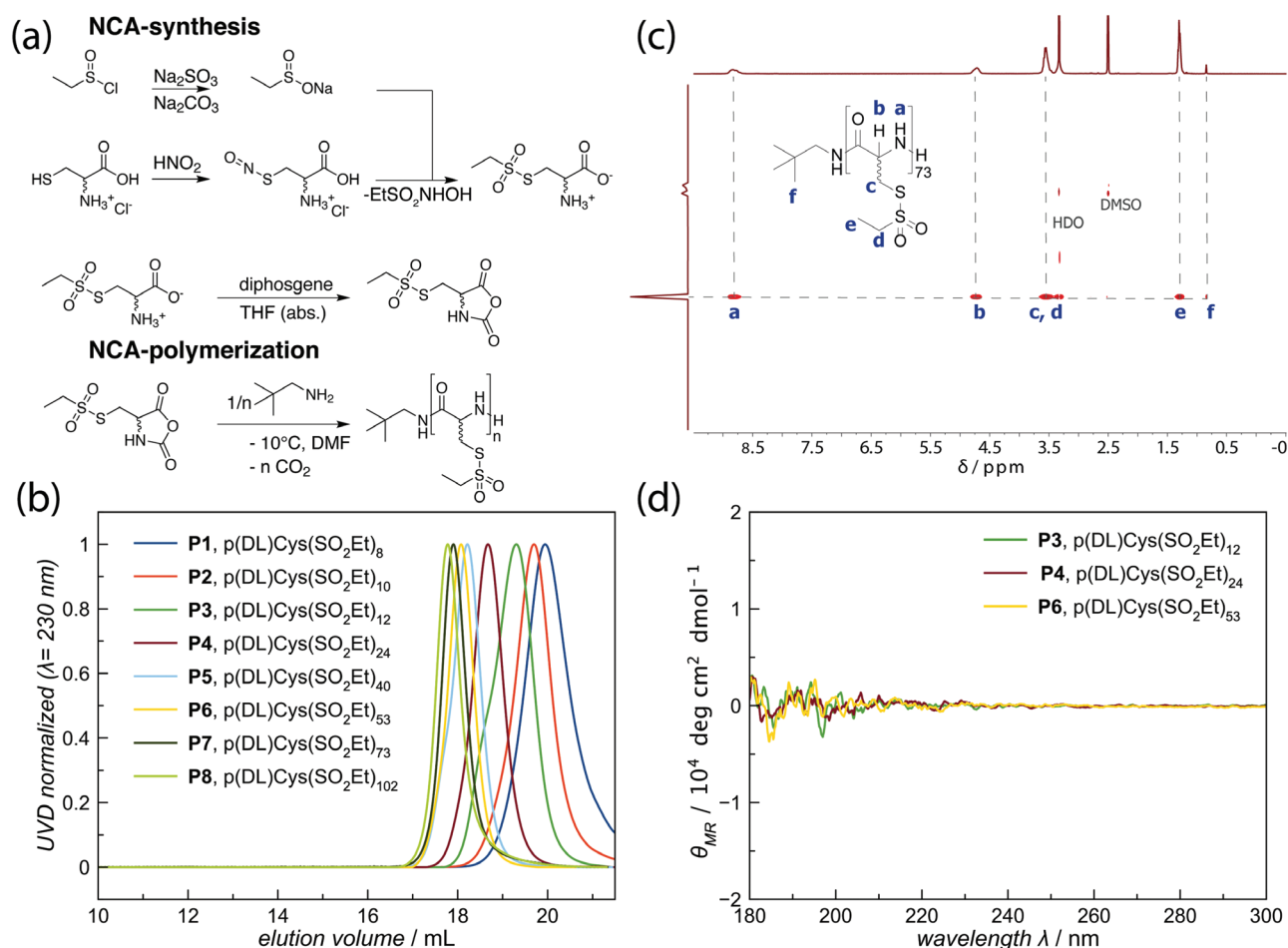


Figure 1. a) Synthesis and ring-opening polymerization of *S*-ethylsulfonyl-*D,L*-cysteine *N*-carboxyanhydride. b) Analytical gel permeation chromatography in hexafluoroisopropanol (HFIP GPC) of P1 to P8 indicates symmetric molecular weight distributions and a clear shift toward higher molecular weights with increasing monomer-to-initiator ratio. c) DOSY NMR for p(DL)Cys(SO₂Et)₇₃ reveals the presence of only a single polymer species. d) CD spectroscopy in hexafluoroisopropanol does not give a prevalent signal irrespective of the polymer chain length, as expected for racemic compounds.

Table 1. Polymerization of *S*-(ethylsulfonyl)-DL-cysteine NCA.

No.	M/I	Conversion ^{a)} [%]	X_n ^{b)}	M_n ^{b)} [kDa]	M_n ^{c)} [kDa]	\bar{D} ^{c)} [kDa]
P1	4	100	8	1.65	2.92	1.31
P2	8	100	10	2.04	4.16	1.22
P3	15	100	12	2.43	6.20	1.21
P4	30	100	24	4.77	10.1	1.20
P5	40	100	40	7.90	18.0	1.24
P6	50	100	53	10.4	20.9	1.19
P7	75	89	73	14.3	23.8	1.27
P8	100	91	102	20.0	25.9	1.33

^{a)}Based on IR spectroscopy; ^{b)}End-group analysis by ¹H NMR; ^{c)}HFIP GPC relative to PMMA standards.

corresponds well with the previously published crystal structure of L-Cys(SO₂Et) NCA.^[36]

ROP of DL-Cys(SO₂Et) NCA was performed at -10 °C in dry and purified *N,N*-dimethyl formamide (DMF) using neopentylamine as initiator (Figure 1a). These conditions have been reported optimal to ensure controlled living polymerization of L-Cys(SO₂Et) NCA, since the *S*-ethylsulfonyl protecting group remains intact during nucleophilic amine-initiated NCA polymerization, but can be used for consecutive disulfide bond formation with soft nucleophile thiols.^[29,37]

For the synthesis of poly(*S*-ethylsulfonyl-DL-cysteine) (p(DL)Cys(SO₂Et)), racemic Cys(SO₂Et) NCA could be polymerized with high conversion rates of 89–100%, according to IR spectroscopy. As summarized in **Table 1**, the intended chain lengths are in well agreement with the results obtained from end-group analysis by NMR, and polypeptides with chain lengths from $X_n = 8$ to 102 with molecular weights up to 20.0 kDa could be successfully synthesized. Analysis by gel permeation chromatography (GPC) in hexafluoroisopropanol (HFIP) shows symmetric and monomodal molecular weight distributions for all polymers with well-defined dispersity ($\bar{D} = 1.19$ –1.33), relative to poly(methyl methacrylate) (PMMA) standards. A clear shift in the elution volume maximum can be detected by GPC, indicating controlled polymerization and valid chain lengths (Figure 1b and Figure S4, Supporting Information). The integrity of the polymer backbone as well as the reactive *S*-ethylsulfonyl protecting group was confirmed by the presence of only a single polymeric species in diffusion ordered spectroscopy (DOSY) NMR (Figure 1c) with all polymer signals being aligned. Furthermore, CD spectroscopy in HFIP verified the racemic nature of the isolated p(DL)Cys(SO₂Et) homopolymers, since no prevalent signal could be detected (Figure 1d).

In comparison to the results published on p(L)Cys(SO₂Et), indeed, longer chain lengths and higher conversion rates could be obtained from the racemic NCA.^[29] For p(L)Cys(SO₂Et), the maximum chain length reported was $X_n = 43$, although, due to the formation of aggregates induced by strong antiparallel β -sheets, multimodal molecular weight distributions were detected in HFIP GPC. While for p(L)Cys(SO₂Et) homopolymers with up to 20 repeating units narrow and symmetric molecular weight distributions were reported, chain lengths above

$X_n = 20$ resulted in asymmetric distributions, which turned multimodal above $X_n = 30$.^[29] In case of p(DL)Cys(SO₂Et), for chain lengths up to $X_n = 102$, symmetric molecular weight distributions and no aggregates were detected by HFIP GPC, thus facilitating polymer analysis and interpretation of the results (see **Table 1** and **Figure 1**). For the synthesis of even higher molecular weights ($M/I = 150$), however, increased tailing was observed, as discussed further below.

To reveal the secondary structure of p(DL)Cys(SO₂Et), the racemic polypeptides were analyzed by IR spectroscopy in solid state. As shown in **Figure 2a**, vibrational amide bands were detected at 1637 cm⁻¹ (amide I), 1509 cm⁻¹ (amide II), and 703 cm⁻¹ (amide V), indicating β -sheet secondary structure, while the weak shoulder at 1702 cm⁻¹ suggests their antiparallel orientation.^[38,39] No chain length dependencies were detected for the general position of the amide bands, whereas the shoulder at 1702 cm⁻¹ becomes more evident with increasing chain lengths. For comparison, p(L)Cys(SO₂Et), which is known to adopt an antiparallel β -sheet structure, shows similar wave numbers for the vibrational amide bands, but a distinct peak at 1702 cm⁻¹ for p(L)Cys(SO₂Et)₁₃ (Figure 2a and Figure S7, Supporting Information, dashed green line).^[29] In conclusion, p(DL)Cys(SO₂Et) seems to adopt β -sheet secondary structure with weakly pronounced antiparallel orientation.^[40,41] In contrast, poly(*S*-ethylsulfonyl-L-homocysteine), bearing the same reactive protecting group, displays chain-length-dependent helix formation (1652 cm⁻¹) in solid state, and a fraction of aggregated protein structure (1625 cm⁻¹) disappears with increasing chain lengths (see **Figure S7**, Supporting Information).

Since IR spectroscopy does not allow for reliable analysis of the polypeptide tacticity, ¹H NMR spectra of racemic p(DL)Cys(SO₂Et) and enantiopure p(L)Cys(SO₂Et) in dimethyl sulfoxide were employed for comparison.^[42,43] In absence of racemization, enantiopure NCAs are known to form isotactic polypeptides, whereas the polymerization of racemic NCA mixtures can be considered a copolymerization, leading to an overall atactic polymer with only short isotactic sequences, unless stereoselective or guiding templates are involved.^[42,44,45] In our case, polymerization is conducted in solution without any additional driving force. As such, the signals of the racemic homopolymers (Figure 2b, upper spectrum) appear to be much broader than those of purely isotactic p(L)Cys(SO₂Et) (Figure 2b, lower spectrum), which suggests the rather atactic nature of the prepared p(DL)Cys(SO₂Et) homopolymers. For a detailed understanding, however, further studies are required.

To gain deeper insight into the polymerization of DL-Cys(SO₂Et) NCA, the kinetic behavior was investigated via IR spectroscopy. The carbonyl stretching bands at 1858 and 1788 cm⁻¹ were monitored over the course of 5 d and the integrals analyzed, which correspond to the monomer concentration.

The majority of NCAs investigated to date (e.g., γ (benzyl)-L-glutamic acid NCA, *N*- ϵ (carbobenzoxy)-L-lysine NCA) are known to adopt an α -helical conformation, after a short initiation period, resulting in pseudo-first-order kinetics in polar solvents (e.g., DMF).^[1,5,20] In contrast, cysteine NCA derivatives are known to form β -sheets upon polymerization.^[20] Exemptions were only reported when large polar (e.g., oligoethylene glycol) or bulky side groups (e.g., menthyl) have been introduced via thioether bonds.^[25,46] Vice versa, during the polymerization of

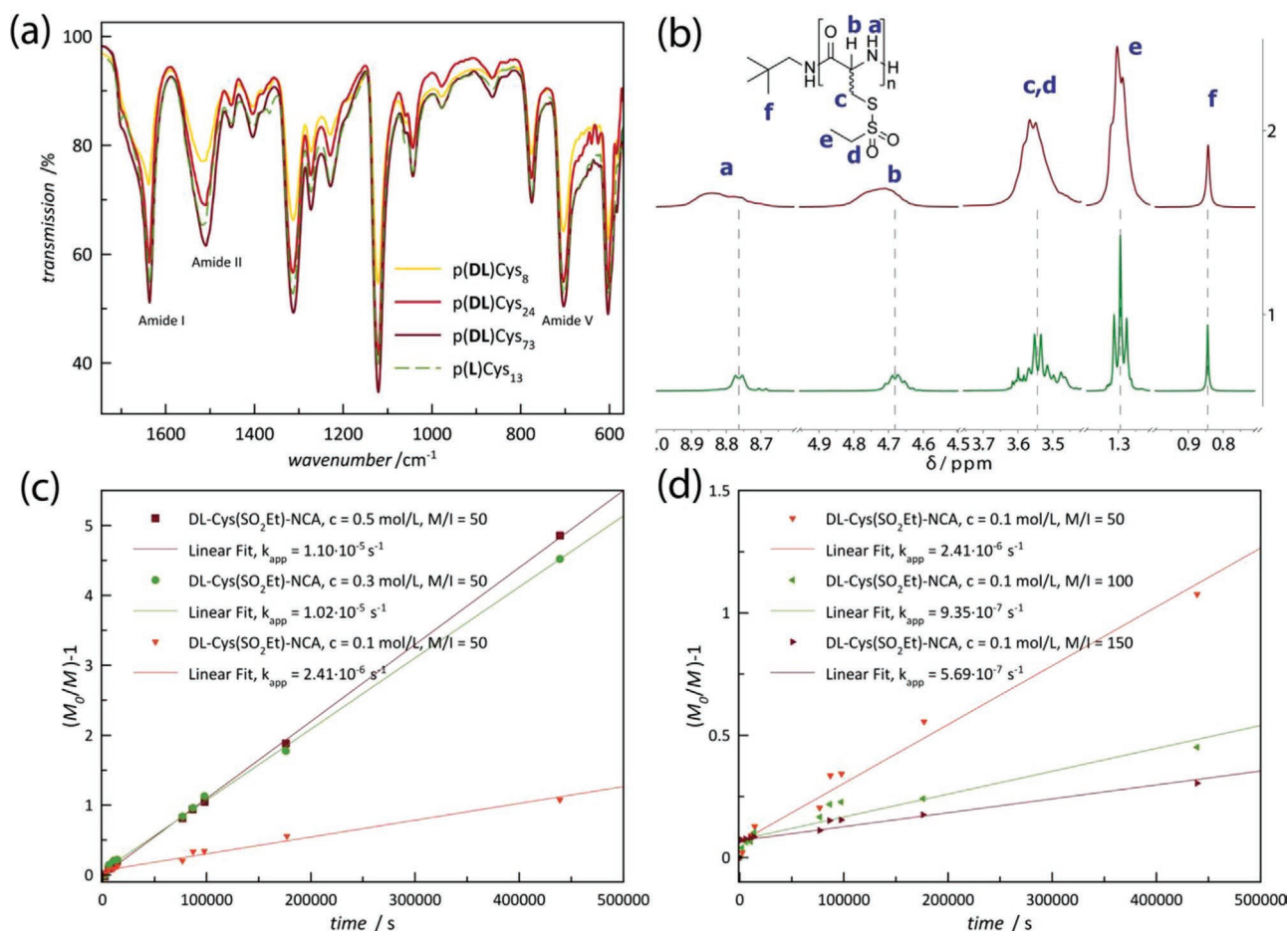


Figure 2. Secondary structure analysis and kinetic investigations. a) Infrared spectroscopy (solid state) of racemic and enantiopure poly(S-ethylsulfonyl cysteine) with chain lengths of 8 to 73. b) NMR spectroscopy of p(DL)Cys(SO₂Et)₂₂ (upper) and p(L)Cys(SO₂Et)₁₇ (lower) in DMSO-d₆. c) Kinetic plot of p(DL)Cys(SO₂Et), M/I = 50 at varying monomer concentrations. d) Kinetic plot of p(DL)Cys(SO₂Et), c_{NCA} = 0.1 mol L⁻¹ with varying monomer-to-initiator ratios.

S-(methyl)-L-cysteine NCA, Kawai and Komoto observed secondary structure-driven crystallization hampering polymerization progress. Instead of first-order kinetics, the polymerization behavior could be described by the Avrami equation.^[12] As suggested by Iguchi, the Avrami equation, originally developed for crystallization kinetics, can be applied to describe a polymerization system which starts as a homogenous mixture but turns heterogeneous throughout polymerization.^[47] No transfer or chemical termination reactions occur, but the association of oligomers leads to soluble (nano)crystallites ultimately leading to physical termination, as the growing chain end loses its mobility. Further growth is only possible at the surface.^[13,47] The adapted Avrami equation is given by^[29,47]

$$\frac{\delta(x)}{\delta(t)} = k [I] [M_0] \left(1 - \frac{x}{[M_0]} \right)^2 \quad (1)$$

with $[M_0]$ is the initial monomer concentration; $[I]$ is initiator concentration; $x = [M_0] - [M_t]$ is the consumed monomer at time t ; and k is the rate constant, and can also be written as^[29]

$$\frac{\delta(x)}{\delta(t)} = k [I] \frac{[M_t]^2}{[M_0]} \quad (2)$$

It can thus be derived as

$$\frac{[M_0]}{[M_t]} = k [I] t + 1 \quad (3)$$

By plotting $\frac{[M_0]}{[M_t]} - 1$ versus the reaction time (t), the apparent

rate constant of the polymerization ($k_{app} = k_p \cdot [I]$) as well as the polymerization rate (k_p) can be calculated. As shown in Figure 2c,d, the experimental values obtained from IR spectroscopy follow the derived linear dependency. At constant monomer-to-initiator ratio, apparent rate constants increase with increasing monomer concentration, and decrease with increasing monomer-to-initiator ratio, when the monomer concentration is kept constant. In a similar manner, the polymerization of L-Cys(SO₂Et) NCA was reported to follow the Avrami model, and both polymerizations seem to be affected by the formation of insoluble crystallites which govern the general polymerization behavior qualitatively.^[29] In contrast,

Table 2. Polymerization kinetics. Apparent rate constants (k_{app}) and rate constants (k_p) for the ring-opening polymerization of *S*-(ethylsulfonyl)-protected NCA monomers.

NCA monomer	c_{NCA} [mol L ⁻¹]	k_{app} [s ⁻¹]	k_p [L mol ⁻¹ s ⁻¹]
DL-Cys(SO ₂ Et)	0.1	2.41×10^{-6}	1.21×10^{-3}
	0.3	1.02×10^{-5}	1.70×10^{-3}
	0.5	1.10×10^{-5}	1.10×10^{-3}
L-Cys(SO ₂ Et) ^{a)}	0.17	3.43×10^{-6}	1.01×10^{-3}
	0.43	8.09×10^{-6}	9.41×10^{-4}
	0.59	1.13×10^{-5}	9.58×10^{-4}
L-Hcy(SO ₂ Et) ^{b)}	0.1	1.44×10^{-5}	7.20×10^{-3}
	0.3	4.33×10^{-5}	7.22×10^{-3}
	0.5	5.29×10^{-5}	5.29×10^{-3}

^{a)}Values taken/calculated from Schäfer et al.^[29]; ^{b)}Values taken/calculated from Muhl et al.^[48]

S-ethylsulfonyl-L-homocysteine (L-Hcy(SO₂Et)) NCA showed fast pseudo-first-order kinetics typically observed for α -helical polymerization.^[48] When comparing the (apparent) rate constants, as summarized in **Table 2**, racemic DL-Cys(SO₂Et) NCA polymerizes slightly faster than L-Cys(SO₂Et) NCA (40% on average). This observation also reflects on the weaker secondary structure indicated by IR spectroscopy (Figure 2a), the increased solubility (HFIP GPC, Figure 1b), the rather atactic polymer structure, as detected by NMR spectroscopy (Figure 2b), as well as the obtained higher molecular weights.

Nevertheless, for DL-Cys(SO₂Et) NCA, the discrepancy among the reaction performed at a monomer concentration of 0.3 mol L⁻¹ versus 0.5 mol L⁻¹ is not significant, and similar conversions were detected for each time point. In agreement with these findings, certain limitations were detected for the polymerization of DL-Cys(SO₂Et) NCA. As shown in Figure S5a (Supporting Information), the monomer concentration has a major impact on the reaction. Polymerizations at high NCA concentration ($\beta_{NCA} = 100$ g L⁻¹, $c_{NCA} = 0.42$ mol L⁻¹) lead to gelation after 50% conversion, resulting in low molecular weight polymers and bimodal GPC elugrams (see also Figure S6, Supporting Information). On the other hand, low NCA concentrations ($\beta_{NCA} = 30$ g L⁻¹, $c_{NCA} = 0.13$ mol L⁻¹) result in slow polymerization progress and only low molecular weight polymers, even though high NCA conversions were achieved after six weeks at -10 °C. Medium NCA concentrations ($\beta_{NCA} = 60$ g L⁻¹, $c_{NCA} = 0.25$ mol L⁻¹) finally granted polymer synthesis up to chain lengths of $X_n = 102$ with well-defined polydispersity index (PDI). However, increased tailing and no significant shift in the maximum elution volume was detected for M/I ratio of 150 (Figure S5b, Supporting Information), even though polymerization was carried out at similar conditions in purified and dry DMF (<50 ppm water). Interestingly, for p(L)Cys(SO₂Et), gelation was not observed until monomer concentrations above 0.8 mol L⁻¹.^[29]

Since we generally found high conversion rates for the polymerization of DL-Cys(SO₂Et) NCA, we aimed to exploit the racemic NCA for the synthesis of block copolypept(o)ides. As illustrated in **Figure 3a**, the triblock copolymer, p(L)Glu(OBn)-*b*-p(DL)Cys(SO₂Et)-*b*-pSar, with poly(*S*-ethylsulfonyl-DL-cysteine) as the middle block, was prepared by sequential NCA addition,

after full conversion of the predecessor monomer was ensured by IR spectroscopy. Of note, due to incomplete conversion, the displayed sequence would require an additional intermediate work-up step if the enantiopure (L)Cys(SO₂Et) NCA was used. The results of the triblock copolymer synthesis are given in Figure 3 and summarized in Table S1 (Supporting Information). As shown, the calculated block lengths are in well agreement with the results obtained from end-group analysis in NMR (Figure 3b). More importantly, symmetric and monomodal molecular weight distributions could be observed for each reaction step by HFIP GPC. The clear shift in the elution volume maximum without significant tailing underlines the controlled living nature of the polymerization. In addition, the final polymers displayed molecular weights of 19 400 g mol⁻¹ (diblock, p(L)Glu(OBn)-*b*-p(DL)Cys(SO₂Et)) and 33 200 g mol⁻¹ (triblock, p(L)Glu(OBn)-*b*-p(DL)Cys(SO₂Et)-*b*-pSar,) as well as well-defined polymer dispersities of 1.23 and 1.43, relative to PMMA standards (see Figure 3c and Table S1, Supporting Information).

Since the individual GPC curves are not baseline-separated, due to the chosen block length values, which are ideal with respect to polypeptide solubility, we investigated the absence of homopolymers by DOSY NMR spectroscopy. As a result of the reduced size of homopolymers, compared to consecutive diblock and triblock copolymers, monomodal peaks at a distinct diffusion index would broaden, become multimodal or, in the case of homopolymers coexisting with triblock copolymers, even two distinct species appear. As displayed in Figure 3d and Figure S18 (Supporting Information), we observed only one diffusing species with narrow diffusion index distribution for diblock as well as triblock copolymers. Therefore, DOSY NMR experiments confirm successful block copolymer synthesis by controlled living ROP, which specifies the applicability of the racemic DL-Cys(SO₂Et) NCA for the synthesis of thiol-reactive block copolymers.

We found that racemic DL-Cys(SO₂Et) NCAs can be successfully prepared and polymerized yielding well-defined homopolymers with symmetric molecular weight distributions for molecular weights up to 20.0 kDa, corresponding to an average degree of polymerization of 102 (determined by end-group analysis). To the best of our knowledge, for polypeptides forming β -sheets, this is the first comprehensive study on the use of racemic NCAs to improve their polymerization. The polymerization of DL-Cys(SO₂Et) NCA follows the Avrami model for heterogeneous polymerization, even though the formation of antiparallel β -sheets was found to seem less pronounced than for purely isotactic p(L)Cys(SO₂Et), resulting in slightly faster polymerization rates and full monomer conversion. As a consequence, the synthesis of triblock copolymers by sequential copolymerization can be achieved with excellent control over individual block lengths. Future research will thus address the question of how a reduced tendency for secondary structure formation affects the solution self-assembly of p(DL)Cys(SO₂Et)-containing block copolymers and the properties of nanoparticles thereof.

Experimental Section

Materials and Methods: Unless stated otherwise, reagents and solvents were purchased from Sigma Aldrich and used as received. THF

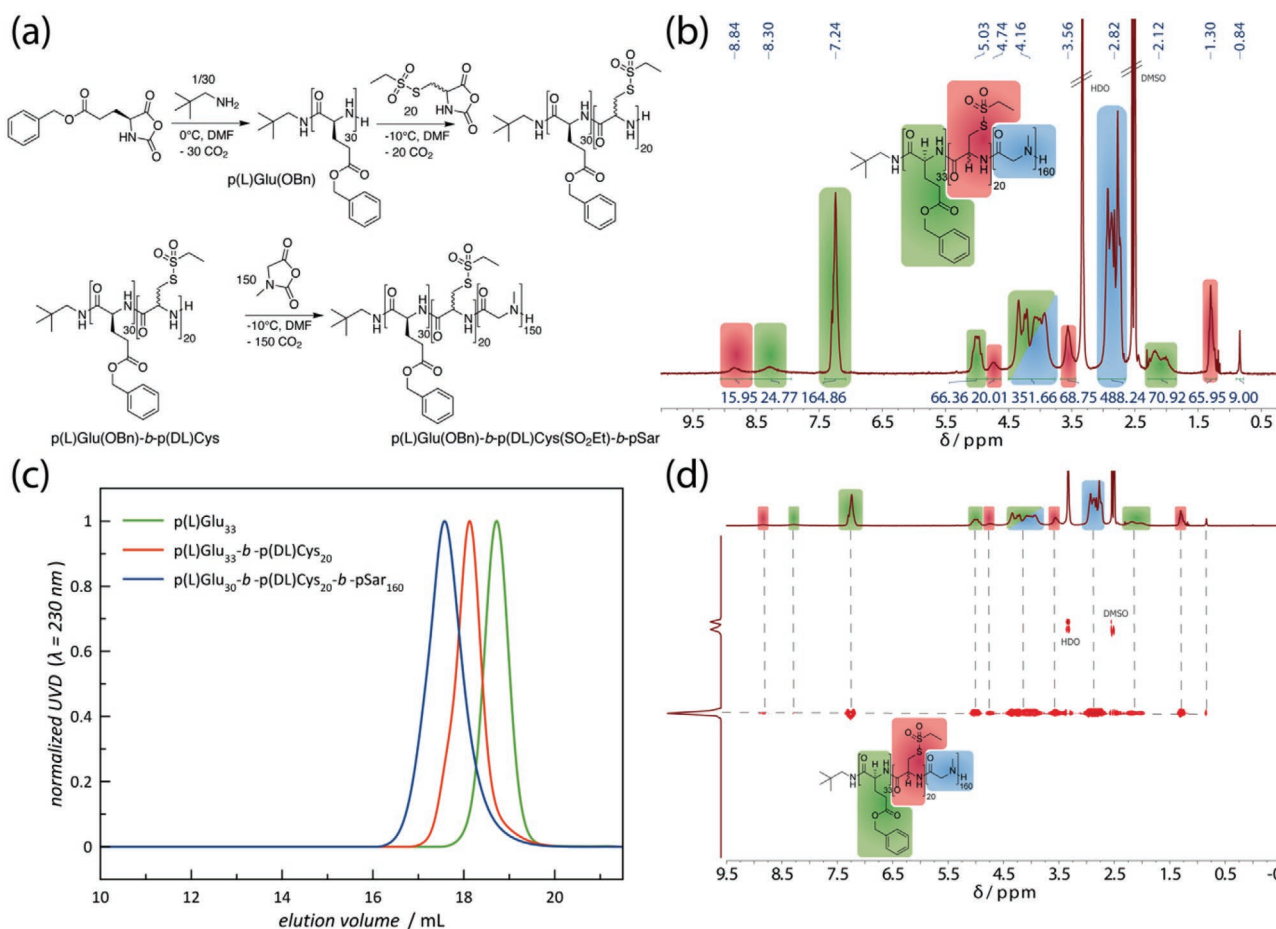


Figure 3. Triblock copolymer synthesis. a) Synthesis of p(L)Glu(OBn)₃₀-b-p(DL)Cys(SO₂Et)₂₀-b-pSar₁₅₀ via sequential NCA polymerization. b) End-group analysis by ¹H NMR spectroscopy. c) Analytical HFIP GPC of the respective block sequences. For better visualization, p(L)Glu and p(DL)Cys were used as abbreviations for p(L)Glu(OBn) and p(DL)Cys(SO₂Et). d) DOSY NMR indicates the presence of only one diffusing polymer species.

was dried over Na and freshly distilled prior to use. DMF was bought from Acros (99.8%, extra dry over molecular sieve) and purified by repetitive freeze-pump-thaw cycles to remove dimethylamine prior to use (water content < 50 ppm). Neopentylamine was purified by distillation over calcium hydride and stored over activated molecular sieves before further use. HFIP was purchased from Fluorochem. Deuterated solvents were obtained from Deutero GmbH and were used as received. ¹H NMR spectra were recorded on a Bruker Avance II 400 at room temperature at a frequency of 400 MHz. DOSY spectra were recorded on a Bruker Avance III HD 400 (400 MHz). Calibration of the spectra was achieved using the solvent signals. NMR spectra were analyzed with MestReNova version 12.0.4 from Mestrelab Research S.L. Degrees of polymerization (X_n) by ¹H NMR were calculated comparing the integral of the initiator peak and the integrals of the α -protons. Attenuated total reflectance Fourier transformed infrared (ATR-FTIR) spectroscopy was performed on a FT/IR-4100 (JASCO Corporation) with an ATR sampling accessory (MIRacle, Pike Technologies). IR spectra were analyzed using Spectra Manager 2.0 (JASCO Corporation). NCA polymerization was monitored by FTIR spectroscopy. Polymerization was judged to be completed when NCA associated carbonyl peaks at 1858 and 1788 cm⁻¹ had vanished. Analytical GPC was performed on a Jasco GPC setup at a flow rate of 0.8 mL min⁻¹ and a temperature of 40 °C. The eluent was HFIP equipped with 3 g L⁻¹ potassium trifluoroacetate. The column material was modified silica gel (PFG columns, particle size: 7 μ m, porosity: 100 and 4000 Å), purchased from PSS Polymer Standards Service GmbH. For polymer detection, a UV detector (Jasco UV-2075+) at a wavelength of λ = 230 nm was employed. Molecular weights were determined by using

a calibration with PMMA (PSS Polymer Standards Services GmbH) with toluene as internal standard. The elution diagram was evaluated with PSS WinGPC (PSS Polymer Standard Service GmbH). Circular dichroism (CD) spectroscopy was performed on a Jasco J-815 spectrometer at room temperature and Spectra Manager 2.0 (Jasco) was used to analyze the spectra. A cell with a path length of 1 mm was used. Spectra were recorded at a concentration of 0.1 g L⁻¹ polymer in HFIP. Θ_{MR} was calculated using the equation with $M_{\text{repeating unit}} = 195.26 \text{ g mol}^{-1}$, $c_M = 0.1 \text{ g L}^{-1}$, and $l = 0.1 \text{ cm}$ for (Cys(SO₂Et))

$$\theta_{MR} = \frac{\theta \cdot M_{\text{repeating unit}}}{10 \cdot l \cdot c_M} \left[\text{deg cm}^2 \text{ d mol}^{-1} \right] \quad (4)$$

Synthesis of Sodium Ethylsulfinate: The synthesis of sodium ethylsulfinate was adapted from literature.^[28]

A solution of sodium sulfite (142.6 g, 1.38 mol, 3.5 eq.) in water (275 mL) was heated to 80 °C. Ethanesulfonyl chloride (37.6 mL, 50.84 g, 0.395 mol, 1.0 eq.) and sodium carbonate (84.09 g, 0.793 mol) were added simultaneously while significant quantities of CO₂ evolved. The reaction mixture was stirred for 1 h at 80 °C. Next, the solvent was removed in vacuo at 40 °C. The resulting solid was suspended in methanol (\approx 300 mL) and filtered to remove sodium carbonate and side products. Evaporation of methanol yielded sodium ethylsulfinate (45.0 g, 0.388 mol, 98%) as a colorless solid.

¹H NMR (400 MHz, D₂O + TFA-d₁), δ [ppm] = 2.32 (q, 3J = 7.6 Hz, 2H, -CH₂-), 1.06 (t, 3J = 7.6 Hz, 3H, -CH₃).

Synthesis of *S*-(ethylsulfonyl)-DL-cysteine: An ice-cold solution of sodium nitrite (9.90 g, 144 mmol, 1.0 eq.) in degassed water (125 mL) was slowly added to a stirred solution of DL-cysteine hydrochloride (22.6 g, 144 mmol, 1.0 eq.) in previously degassed 2 N HCl (150 mL) at a temperature of 0 °C. After 1 h, sodium ethylsulfinate (44.5 g, 388 mmol, 2.7 eq.) was added to the deep red solution in one portion. After 5 min, a colorless solid precipitated. The suspension was stirred for additional 5 h at 0 °C and was stirred at room temperature overnight. The precipitate was collected and washed with methanol to remove residual sulfinate. The product was dried in vacuo yielding *S*-(ethylsulfonyl)-DL-cysteine (13.5 g, 63.3 mmol, 44%) as a colorless powder.

¹H NMR (400 MHz, D₂O + TFA-*d*₁), δ [ppm] = 4.44 (dd, ³J = 6.7 Hz, ³J = 4.5 Hz, 1H, α -CH), 3.72 (dd, ²J = 15.6 Hz, ³J = 4.5 Hz, 1H, -CH₂-CH-), 3.58 (dd, ²J = 15.6 Hz, ³J = 6.7 Hz, 1H, -CH₂-CH-), 3.50 (dq, ³J = 7.3 Hz, ³J = 1.66 Hz, 2H, -CH₂-CH₃), 1.39 (t, ³J = 7.3 Hz, 3H, -CH₃).

Synthesis of *S*-(ethylsulfonyl)-DL-cysteine *N*-Carboxyanhydride: *S*-(Ethylsulfonyl)-DL-cysteine (7.00 g, 32.82 mmol) was dried by azeotropic distillation with toluene. Next, the amino acid was suspended in absolute THF (100 mL) and diphosgene (3.60 mL, 5.84 g, 29.52 mmol) was added slowly. The suspension was stirred at room temperature until a clear solution was obtained (\approx 3 h). To remove excess diphosgene, a stream of dry nitrogen was led through the reaction mixture into gas washing bottles, equipped with an aqueous NaOH solution, for 2 h. The remaining solvent was removed in vacuo and the residue was dissolved in dry dioxane. Any insoluble compounds were removed by filtration avoiding contact with air, and the NCA solution was slowly precipitated into a mixture of absolute diethyl ether/*n*-hexane (1:2). The precipitation of the product was repeated two more times yielding *S*-(ethylsulfonyl)-DL-cysteine NCA (6.43 g, 26.87 mmol, 82%) as a colorless powder. Absence of chloride impurities was verified by silver nitrate chloride test. mp = 88.5 °C at a heating rate of 7 °C min⁻¹, 86.1 °C at 5 °C min⁻¹ under decomposition.

¹H NMR (400 MHz, D₂O + TFA-*d*₁), δ [ppm] = 9.34 (bs, 1H, NH), 4.85 (ddd, ³J = 5.7 Hz, ³J = 5.2 Hz, ³J = 1.3 Hz, 1H, α -CH), 3.62 (m, 4H, -CH₂-CH- and -CH₂-CH₃), 1.29 (t, ³J = 7.2 Hz, 3H, -CH₃).

For crystallization, dry *n*-hexane was added very carefully on top of an NCA solution in dry ethyl acetate and kept at -20 °C until the formation of colorless NCA crystals was completed.

Synthesis of Poly(*S*-ethylsulfonyl-DL-cysteine): DL-Cys(SO₂Et) NCA (54.8 mg, 229 μ mol, 75 eq.) was transferred into a dried Schlenk flask, dissolved in 0.78 mL of anhydrous DMF (freshly purified by freeze-thaw cycles) and cooled to -10 °C. Neopentylamine initiator (0.266 mg, 3.05 μ mol, 1.0 eq.) was added as a stock solution in DMF (133 μ L, $\beta_{\text{NPA}} = 2.0 \text{ g L}^{-1}$) yielding the reaction mixture with a final NCA concentration of 60 g L⁻¹. A steady flow of dry nitrogen was sustained during the polymerization. The progress of the polymerization was monitored via FTIR spectroscopy and judged to be completed when the carbonyl stretching bands of the NCA at 1858 and 1788 cm⁻¹ had vanished. Samples were taken using a nitrogen flushed syringe through a septum. Upon completed monomer conversion, the polymer was precipitated in a mixture of cold diethyl ether and THF (1:1, v/v). The suspension was centrifuged (4500 rpm, 15 min, 4 °C) and decanted. This procedure was repeated twice concluding with pure diethyl ether. The product was dried in vacuo yielding poly(*S*-ethylsulfonyl-DL-cysteine) (45 mg, 100%) as a colorless to slightly yellow solid.

Polymerizations conducted at lower NCA concentrations ($\beta_{\text{NCA}} = 30 \text{ g L}^{-1}$) resulted in slow polymerization progress, whereas higher NCA concentrations ($\beta_{\text{NCA}} = 100 \text{ g L}^{-1}$) resulted in gelation, yielding low molecular weight polymers for both cases, and polymerization at ($\beta_{\text{NCA}} = 60 \text{ g L}^{-1}$) appears to be optimal.

¹H NMR (400 MHz, DMSO-*d*₆), δ [ppm] = 8.84 (b s, 1n H, NH), 4.71 (b s, 1n H, α -H), 3.57 (b s, 4n H, -CH₂-CH- and -CH₂-CH₃), 1.30 (b s, 3n H, -CH₃), 0.84 (b s, 9H, -(CH₃)₃).

Kinetic Investigations: Polymerizations were prepared as described above and analyzed over a period of 5 d. Samples were taken using a nitrogen flushed syringe through a septum. The decreasing NCA carbonyl peaks at 1858 and 1788 cm⁻¹ were monitored and the integrals were correlated with the NCA concentration for kinetic evaluations.^[49]

Synthesis of *p*(L)Glu(OBn)_{*n*}-*b*-*p*(DL)Cys(SO₂Et)_{*m*}-*b*-*p*Sar_{*o*}: Additional *N*-carboxyanhydride monomers, sarcosine NCA and γ -benzyl-L-glutamate NCA, were prepared according to previous publications.^[31,36]

L-Glu(OBn) NCA (240 mg, 912 μ mol, 30 eq.) was transferred into a predried Schlenk flask, dissolved in 2.0 mL of anhydrous DMF and cooled to 0 °C. Neopentylamine initiator (2.65 mg, 30.4 μ mol, 1.0 eq.) was added as a stock solution in DMF (265 μ L, $\beta_{\text{NPA}} = 10.0 \text{ g L}^{-1}$) and a steady flow of dry nitrogen was sustained during the polymerization. After 3 d, upon completed L-Glu(OBn) NCA conversion, as detected by FTIR spectroscopy, the reaction mixture was cooled to -10 °C and DL-Cys(SO₂Et) NCA (145 mg, 608 μ mol, 20 eq.) was added as a stock solution in anhydrous DMF (72.5 μ L, $\beta_{\text{NCA}} = 200 \text{ g L}^{-1}$). Upon completed DL-Cys(SO₂Et) NCA conversion after additional 6 d, sarcosine NCA (525 mg, 4.56 mmol, 150 eq.) was added as a stock solution in DMF (1.75 mL, $\beta_{\text{NCA}} = 300 \text{ g L}^{-1}$) and the polymerization continued at -10 °C. The reaction was judged to be completed after polymerization for further 19 d, with a total duration of 28 d. Next, the polymer was precipitated into THF. The suspension was centrifuged (4500 rpm, 15 min, 4 °C) and decanted. This procedure was repeated twice concluding with pure diethyl ether. For further purification, the polymer was dialyzed against MilliQ water (MWCO 6–8 kDa) for 1 d and obtained as a colorless powder (385 mg, 58%) from lyophilization of the aqueous solution. For polymer analytics, samples (each 150 μ L) were taken by syringe through the septum, after completion of the respective blocks, and precipitated in THF and diethyl ether as described above.

¹H NMR *p*(L)Glu(OBn)_{*n*} (400 MHz, DMSO-*d*₆), δ [ppm] = 8.30 (b s, 1n H, NH), 7.24 (b s, 5n H, Arom. CH), 5.03 (m, 2n H, O-CH₂), 3.92 (m, 1n H, α -CH), 2.29–1.85 (m, 4n H, β -CH₂- and γ -CH₂-), 0.84 (b s, 9H, -(CH₃)₃).

¹H NMR *p*(L)Glu(OBn)_{*n*}-*b*-*p*(DL)Cys(SO₂Et)_{*m*} (400 MHz, DMSO-*d*₆), δ [ppm] = 8.84 (b s, 1m H, NH), 8.30 (b s, 1n H, NH), 7.24 (b s, 5n H, Arom. CH), 5.03 (m, 2n H, O-CH₂), 4.74 (b s, 1m H, α -CH), 3.92 (m, 1n H, α -CH), 3.57 (b s, 4m H, β -CH₂ and -CH₂-CH₃), 2.29–1.85 (m, 4n H, β -CH₂- and γ -CH₂-), 1.30 (m, 3o H, -CH₃), 0.84 (b s, 9H, -(CH₃)₃).

¹H NMR *p*(L)Glu(OBn)_{*n*}-*b*-*p*(DL)Cys(SO₂Et)_{*m*}-*b*-*p*Sar_{*o*} (400 MHz, DMSO-*d*₆), δ [ppm] = 8.84 (b s, 1m H, NH), 8.30 (b s, 1n H, NH), 7.24 (b s, 5n H, Arom. CH), 5.03 (m, 2n H, O-CH₂), 4.74 (b s, 1m H, α -CH), 4.50–3.77 (m, 1n H + 2p H, α -CH and CH₂), 3.57 (b s, 4m H, -CH₂-CH- and -CH₂-CH₃), 3.07–2.67 (m, 3o H, -CH₃), 2.29–1.85 (m, 4n H, β -CH₂- and γ -CH₂-), 1.30 (m, 3o H, -CH₃), 0.84 (b s, 9H, -(CH₃)₃).

CCDC 2002425 contains the supplementary crystallographic data for this paper. These data can be obtained free of charge from the Cambridge Crystallographic Data Centre via www.ccdc.cam.ac.uk/data_request/cif.

Supporting Information

Supporting Information is available from the Wiley Online Library or from the author.

Acknowledgements

The authors acknowledge funding by the Collaborative Research Center (SFB 1066-2). T.A.B. would like to thank the HaVo Foundation and acknowledge support by the Max Planck Graduate Center (MPGC). Furthermore, the authors would like to thank Lydia Zengerling for supporting the CD spectroscopy measurements.

Conflict of Interest

The authors declare no conflict of interest.

Keywords

NCA polymerization, polypeptides, polypept(o)ides, racemic amino acids, ring-opening polymerization

Received: August 21, 2020
Revised: September 19, 2020
Published online:

-
- [1] H. R. Kricheldorf, *Angew. Chem., Int. Ed.* **2006**, *45*, 5752.
[2] A. Birke, J. Ling, M. Barz, *Prog. Polym. Sci.* **2018**, *81*, 163.
[3] J. Huang, A. Heise, *Chem. Soc. Rev.* **2013**, *42*, 7373.
[4] C. Bonduelle, *Polym. Chem.* **2018**, *9*, 1517.
[5] M. Szwarc, *Adv. Polym. Sci.* **1965**, *4*, 1.
[6] J. Cheng, T. J. Deming, *Pept. Mater.* **2011**, *1*.
[7] D. Huesmann, A. Birke, K. Klinker, S. Türk, H. J. Räder, M. Barz, *Macromolecules* **2014**, *47*, 928.
[8] T. Aliferis, H. Iatrou, N. Hadjichristidis, *Biomacromolecules* **2004**, *5*, 1653.
[9] R. D. Lundberg, P. Doty, *J. Am. Chem. Soc.* **1957**, *79*, 3961.
[10] R. Baumgartner, H. Fu, Z. Song, Y. Lin, J. Cheng, *Nat. Chem.* **2017**, *9*, 614.
[11] C. Chen, H. Fu, R. Baumgartner, Z. Song, Y. Lin, J. Cheng, *J. Am. Chem. Soc.* **2019**, *141*, 8680.
[12] T. Kawai, T. Komoto, *J. Cryst. Growth* **1980**, *48*, 259.
[13] T. Komoto, M. Oya, T. Kawai, *Macromol. Chem.* **1974**, *175*, 301.
[14] H. R. Kricheldorf, C. von Lossow, G. Schwarz, *Macromol. Chem. Phys.* **2004**, *205*, 918.
[15] T. Komoto, M. Oya, T. Kawai, *Macromol. Chem.* **1974**, *175*, 283.
[16] H. R. Kricheldorf, M. Mutter, F. Maser, D. Müller, H. Förster, *Biopolymers* **1983**, *22*, 1357.
[17] P. Y. Chou, G. D. Paman, *Biochemistry* **1974**, *13*, 211.
[18] H. R. Kricheldorf, *Angew. Chem.* **2006**, *118*, 5884.
[19] H. R. Kricheldorf, C. V. Lossow, G. Schwarz, *Macromolecules* **2005**, *38*, 5513.
[20] T. J. Deming, *Chem. Rev.* **2016**, *116*, 786.
[21] T. Akaike, Y. Aogaki, S. Inoue, *Biopolymers* **1975**, *14*, 2577.
[22] D. Huesmann, K. Klinker, M. Barz, *Polym. Chem.* **2017**, *8*, 957.
[23] J. Hwang, T. J. Deming, *Biomacromolecules* **2001**, *2*, 17.
[24] T. Hayakawa, M. Matsuyama, K. Inouye, *Polymer* **1977**, *18*, 854.
[25] T. Hayakawa, Y. Kondo, M. Matsuyama, *Polymer* **1976**, *17*, 1009.
[26] A. Berger, J. Noguchi, E. Katchalski, *J. Am. Chem. Soc.* **1956**, *78*, 4483.
[27] L. B. Poole, F. Radic, *Biol. Med.* **2015**, *80*, 148.
[28] O. Schäfer, D. Huesmann, C. Muhl, M. Barz, *Chem. - Eur. J.* **2016**, *22*, 18085.
[29] O. Schäfer, D. Huesmann, M. Barz, *Macromolecules* **2016**, *49*, 8146.
[30] K. Klinker, M. Barz, *Macromol. Rapid Commun.* **2015**, *36*, 1943.
[31] A. Birke, D. Huesmann, A. Kelsch, M. Weilbacher, J. Xie, M. Bros, T. Bopp, C. Becker, K. Landfester, M. Barz, *Biomacromolecules* **2014**, *15*, 548.
[32] K. Klinker, O. Schäfer, D. Huesmann, T. Bauer, L. Capelôa, L. Braun, N. Stergiou, M. Schinnerer, A. Dirisala, K. Miyata, K. Osada, H. Cabral, K. Kataoka, M. Barz, *Angew. Chem., Int. Ed.* **2017**, *56*, 9608.
[33] A. C. Farthing, R. J. W. Reynolds, *Nature* **1950**, *165*, 647.
[34] F. Fuchs, *Chem. Ber./Recl.* **1922**, *55B*, 2943.
[35] C. Fetsch, A. Grossmann, L. Holz, J. F. Nawroth, R. Luxenhofer, *Macromolecules* **2011**, *44*, 6746.
[36] O. Schäfer, D. Schollmeyer, A. Birke, R. Holm, K. Johann, C. Muhl, C. Seidl, B. Weber, M. Barz, *Tetrahedron Lett.* **2019**, *60*, 272.
[37] M. Barz, D. Huesmann, O. Schäfer, T. Reuter, A. Birke, P. Heller, *WO2015169908A1*, **2014**.
[38] J. T. Pelton, L. R. McLean, *Anal. Biochem.* **2000**, *277*, 167.
[39] E. Goormaghtigh, J. M. Ruyschaert, V. Raussens, *Biophys. J.* **2006**, *90*, 2946.
[40] L. Pauling, R. B. Corey, *Proc. Natl. Acad. Sci. USA* **1953**, *39*, 253.
[41] J. S. Nowick, *Acc. Chem. Res.* **2008**, *41*, 1319.
[42] H. R. Kricheldorf, D. Müller, *Polym. Bull.* **1983**, *10*, 513.
[43] Y. E. Shapiro, *Bull. Magn. Reson.* **1985**, *7*, 27.
[44] I. Rubinstein, R. Eliash, G. Bolbach, I. Weissbuch, M. Lahav, *Angew. Chem.* **2007**, *119*, 3784.
[45] I. Weissbuch, R. A. Illos, G. Bolbach, M. Lahav, *Acc. Chem. Res.* **2009**, *42*, 1128.
[46] X. Fu, Y. Shen, W. Fu, Z. Li, *Macromolecules* **2013**, *46*, 3753.
[47] M. Iguchi, *J. Polym. Sci., Part A-1: Polym. Chem.* **1970**, *8*, 1013.
[48] C. Muhl, O. Schäfer, T. Bauer, H.-J. Räder, M. Barz, *Macromolecules* **2018**, *51*, 8188.
[49] M. Idelson, E. R. Blout, *J. Am. Chem. Soc.* **1957**, *79*, 3948.